

Supplementary information

The search for a unique Raman signature of amyloid beta plaques in human brain tissue from Alzheimer's disease patients.

Benjamin Lochocki¹, Tjado H. J. Morrema², Frek Ariese¹, Jeroen J. M. Hoozemans², Johannes F. de Boer¹

- 1) Department of Physics and Astronomy, LaserLaB Amsterdam, VU Amsterdam, The Netherlands
- 2) Department of Pathology, Amsterdam Neuroscience, Amsterdam University Medical Center, Amsterdam,

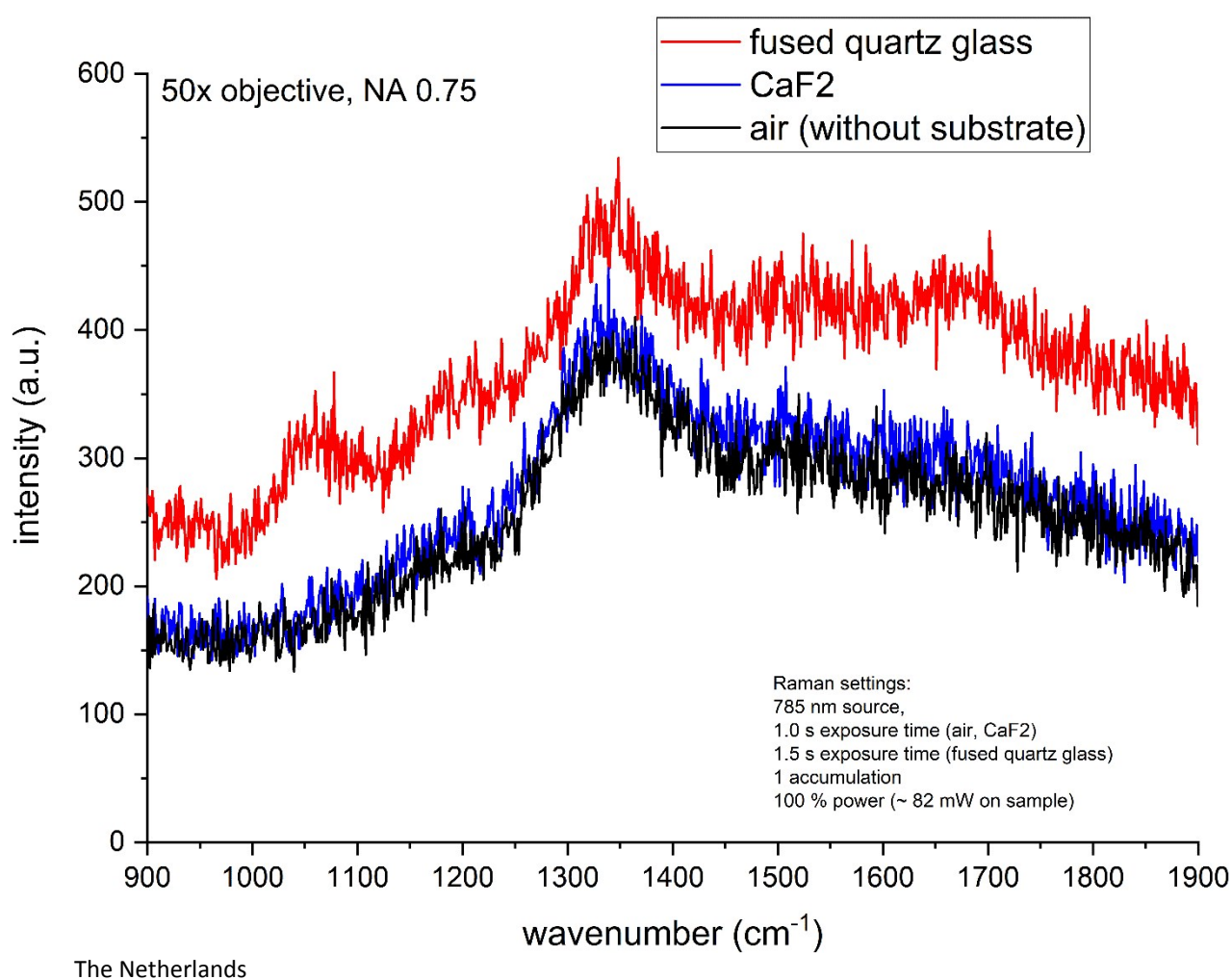


Figure S1: Raman background spectra of the Leica, 50x, 0.75NA, N PLAN EPI objective. Signal coming mainly from the objective (no sample, black line). Similar, but stronger background signal when using fused quartz glass (red line). When using CaF2 substrate, the spectrum (blue line) is practically identical to the measurement without substrate (black line). However, all spectra show a hump around 1350 cm⁻¹ (~ 878 nm), clearly coming from the objective.

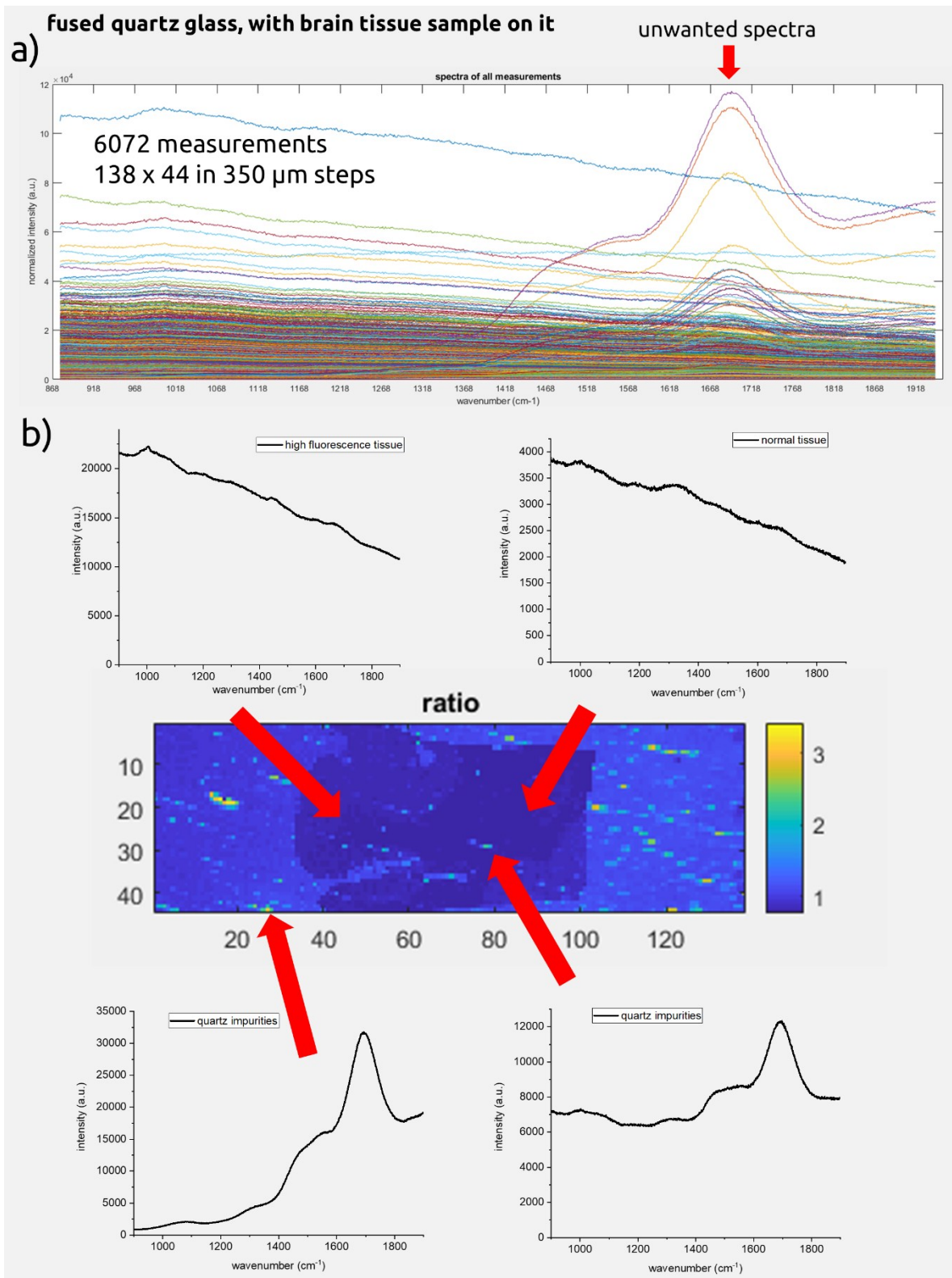


Figure S2: Raman mapping of fused quartz glass substrate (Alfa Aesar) with brain tissue. a) All Raman spectra. b) In the Raman ratio map ($1662\text{cm}^{-1} / 1445\text{cm}^{-1}$) the Raman signal from the substrate is superimposed on the signal from the tissue and clearly visible through the tissue (bright spots). The red arrows indicate the areas where sample spectra were taken to display the spectral variations. To demonstrate that the impurity signal contaminates the tissue signal the lower right graph is shown.

intensity images at wavenumber $1662 \pm 10 \text{ cm}^{-1}$

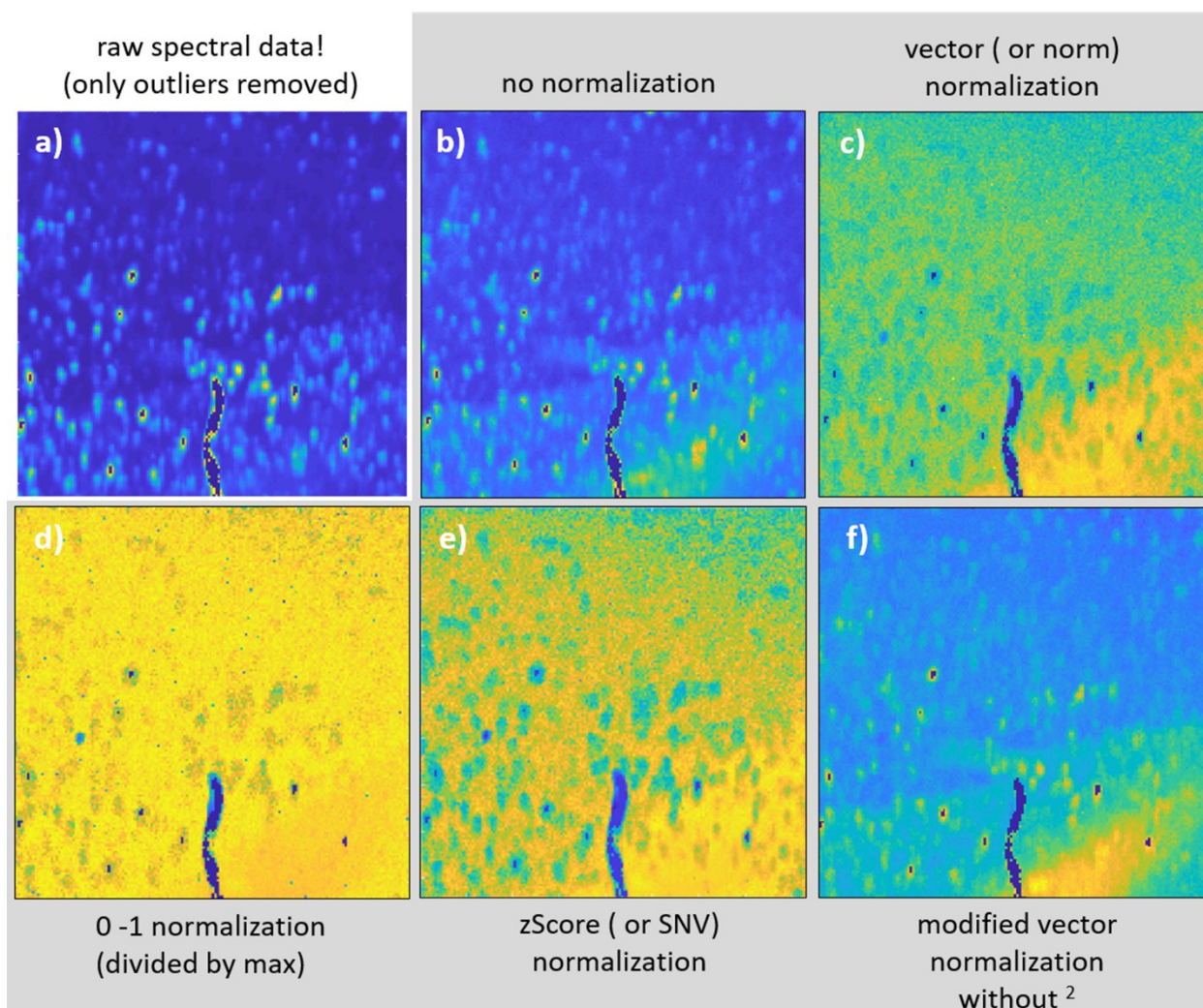


Figure S3: Intensity images at 1662 cm^{-1} following various normalization methods. The data processing for all graphs is the same until normalization: outliers removed (dark blue spots); smoothed (window size 4, rlowess); 6th order polynomial baseline; smoothed (window size 8, rlowess). Color scale: yellow indicates high intensity, dark blue means low intensity (Dark blue spots are mainly where the detector was saturated and hence the data was set to '0'). a) Raw data, no normalization. b) After data processing, no normalization. c) Vector (or norm) normalization. d) Range normalization (divided by max. value). e) SNV or zScore normalization. f) modified vector (or norm) normalization (modified by removing the square part when calculating the 'norm').

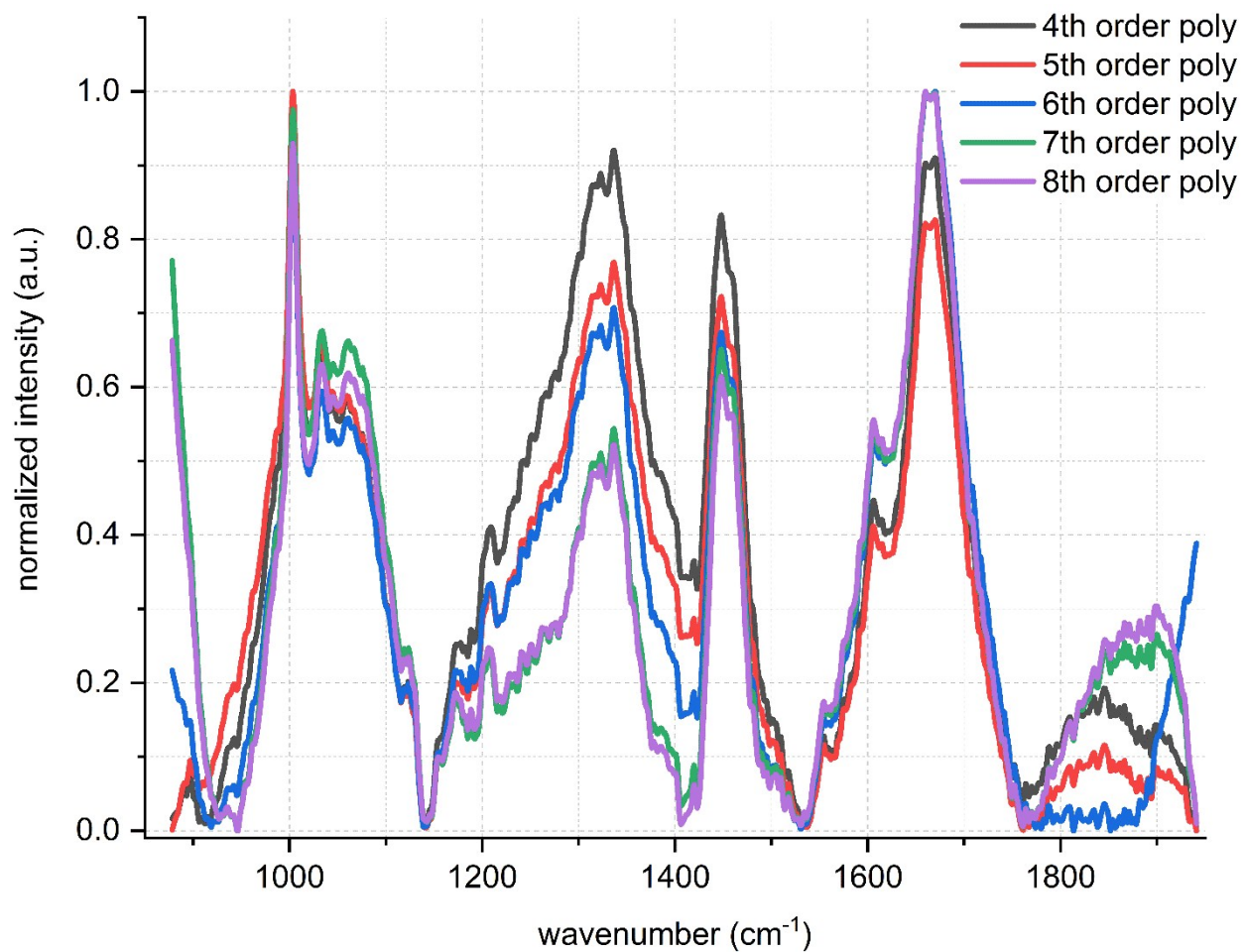


Figure S4: Comparison of the resulting spectra when different polynomials are chosen for the automatic baseline removal. The Raman peak positions are identical and only alter in intensity. The data presented are real averaged measurements, taken from 'normal' tissue.

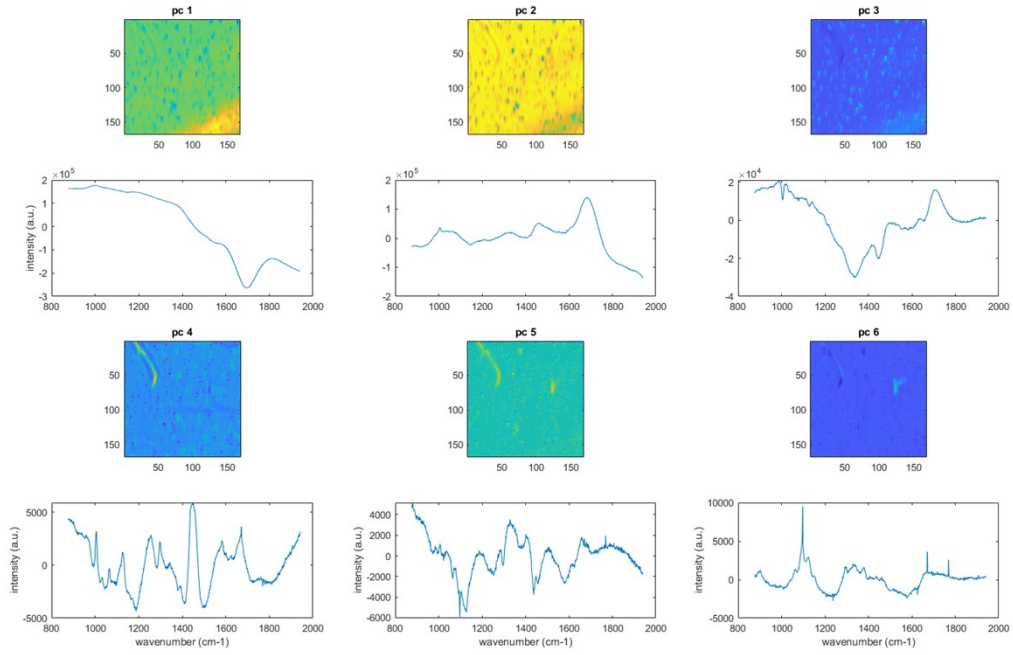


Figure S5: PCA on raw data. Components 1 and 2 are mainly due to the quartz impurities described in Figure S3. Component 3 picks up the fluorescent spots. Components 4 to 6 match partially with some plaque locations but highlight mainly the blood vessel and some calcification spots (pc 4) as can be found in the corresponding bright field image (Figure 1 in the manuscript). The same is valid for pc 6, which is probably debris even though it is positively stained with Thioflavin. Color scale: yellow indicates high intensity, dark blue means low intensity. Image scale: $168 \times 168 \text{ px} = 501 \times 501 \mu\text{m}$.

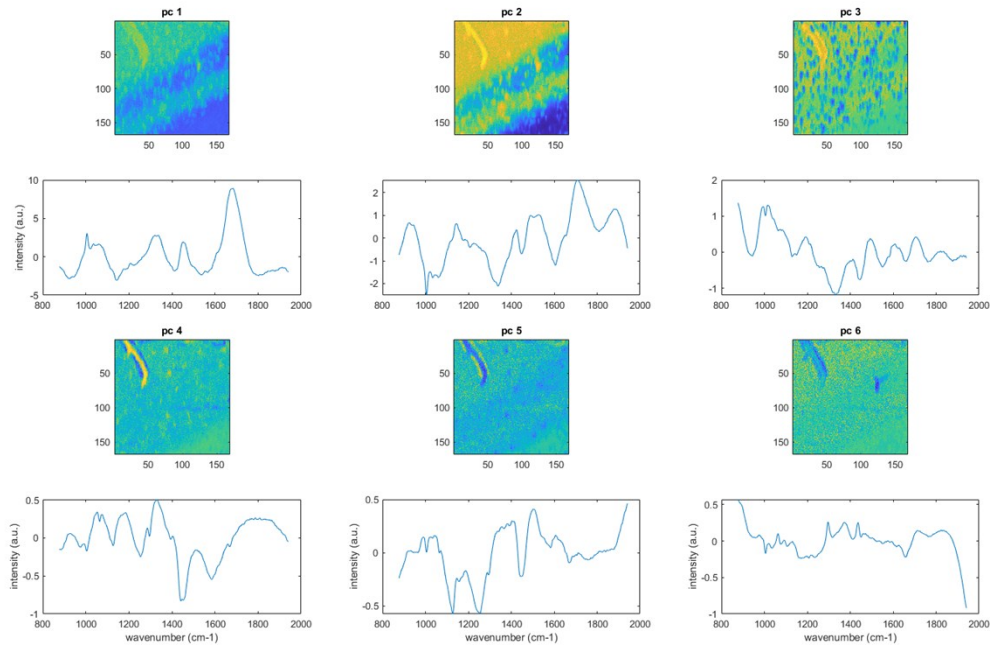


Figure S6: PCA on the same data as Fig. S5 but after smoothing, 6th order polynomial baseline removal, smoothing and vector normalization. Similar results as the PCA analysis of the underlying raw data. For details, see the caption of Figure S5 above. Color scale: yellow indicates high intensity, dark blue means low intensity. Image scale: $168 \times 168 \text{ px} = 501 \times 501 \mu\text{m}$.

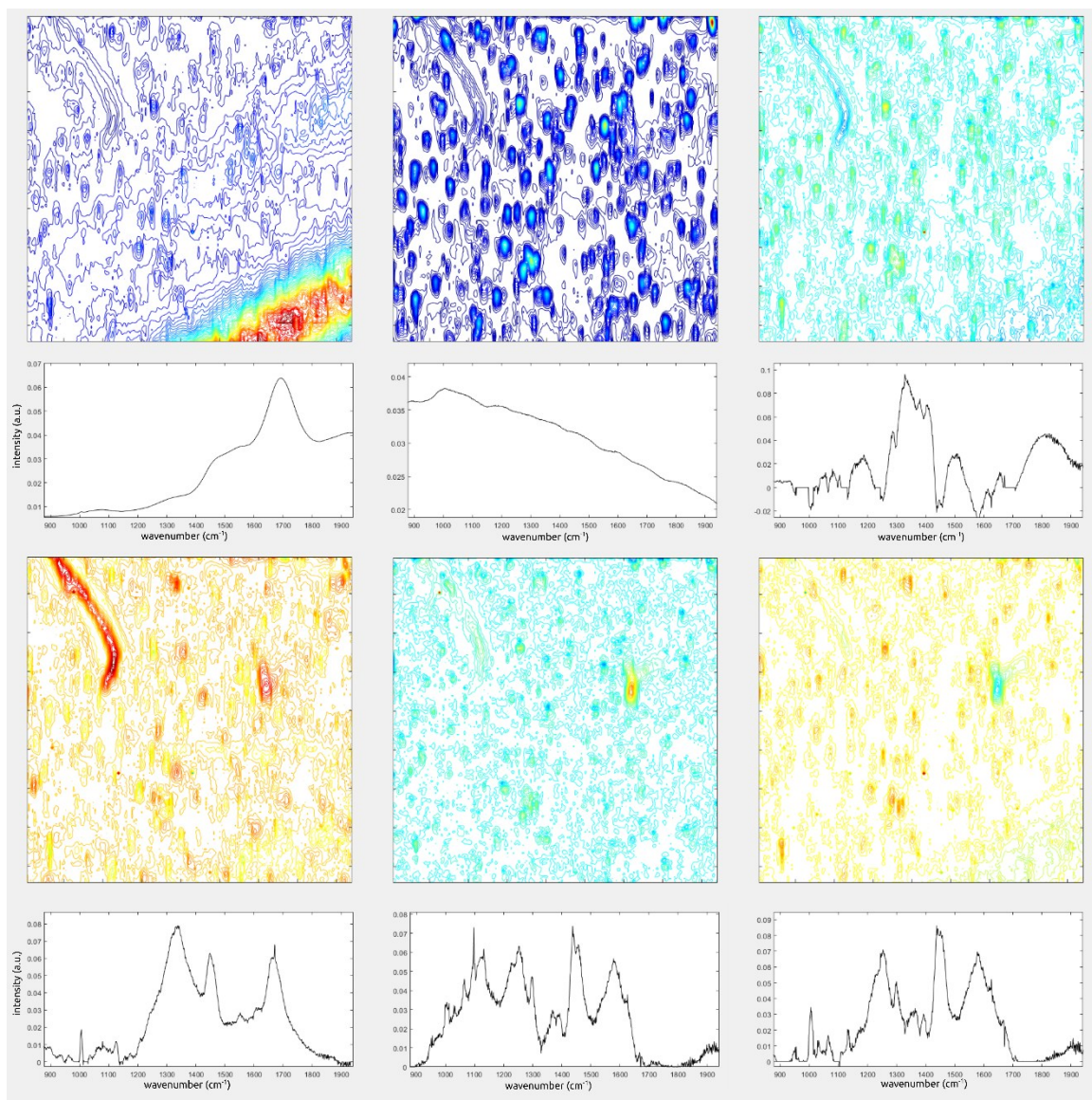


Figure S7: Spectral and contour image results using the *mcr_toolbox2*^{1,2}. Five SVD values were selected, 10% noise was allowed for the pre initial variable detection. Constraints in the column mode were non-negativity (*finnis*). The spectra were normalized using the Euclidean norm and results were obtained after 20 iterations. Applied to the data obtained after: smoothing, baseline removal, additional smoothing and vector normalization. R^2 to explain the percent of variance was: 99.988. The components are ordered from top left to bottom right. The obtained results are similar in terms of structural locations compared to the results from the principal component analysis in Figure S6. The first component represents the impurities from the substrate; the second component highlights the fluorescent spots. However, spectra and loadings in Figures S5, S6 and S7 do not show a unique plaque correlated output. Color scale: yellow indicates high intensity, dark blue means low intensity. Image scale: 168 x 168 px = 501 x 501 μm .

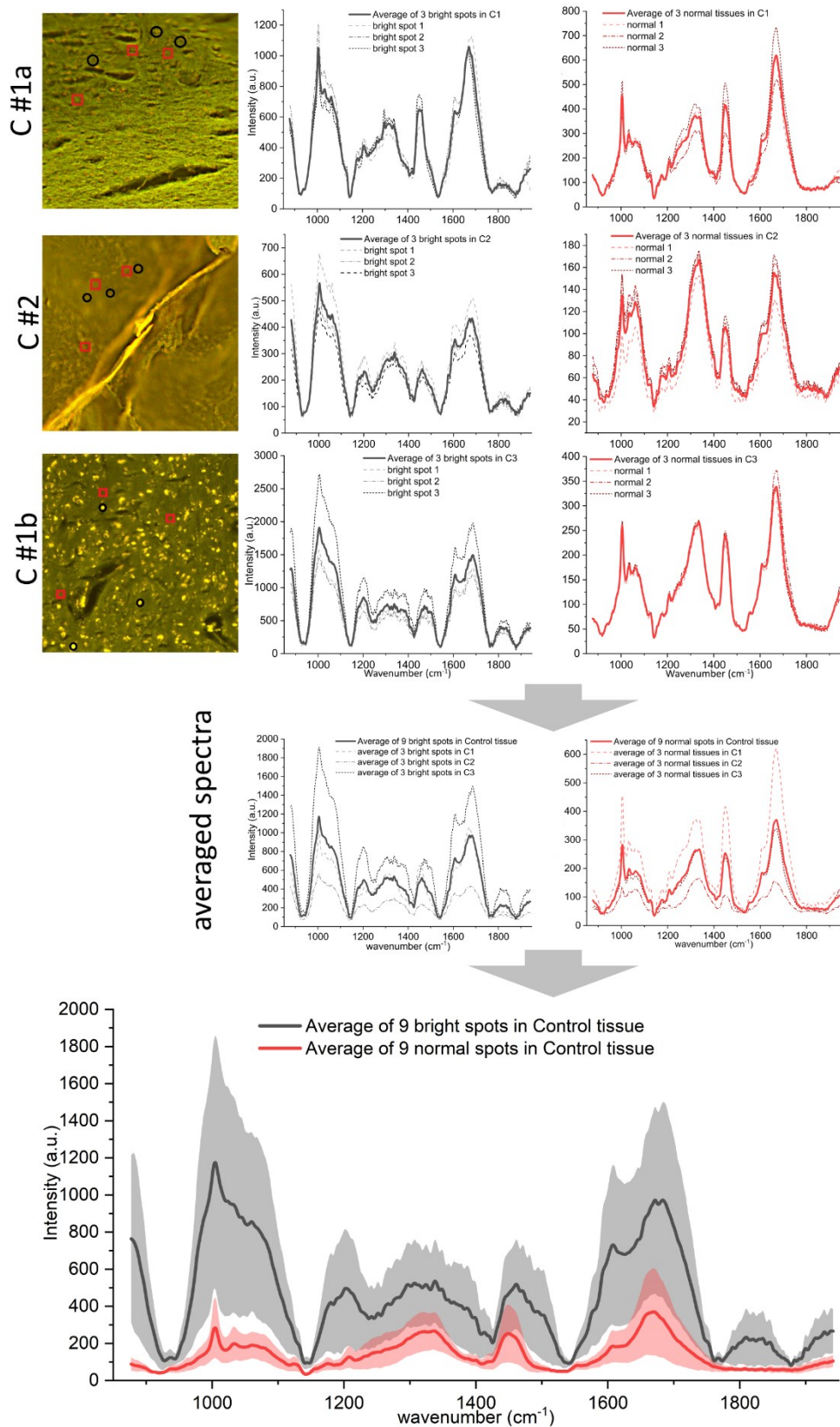


Figure S8: Raman spectra taken from the three healthy control samples, similar conditions and data processing as to the AD cases in Figure 4 in the main manuscript. Black solid lines are the average spectra of three averaged spectra (dashed black line) taken from bright spot areas (3x3 pixels). The red lines are the spectra taken from 'normal' background tissue (red squares). In the graph at the bottom, both averages are plotted with their standard deviation. It is also the basis of the comparison presented in the manuscript as Figure 7.

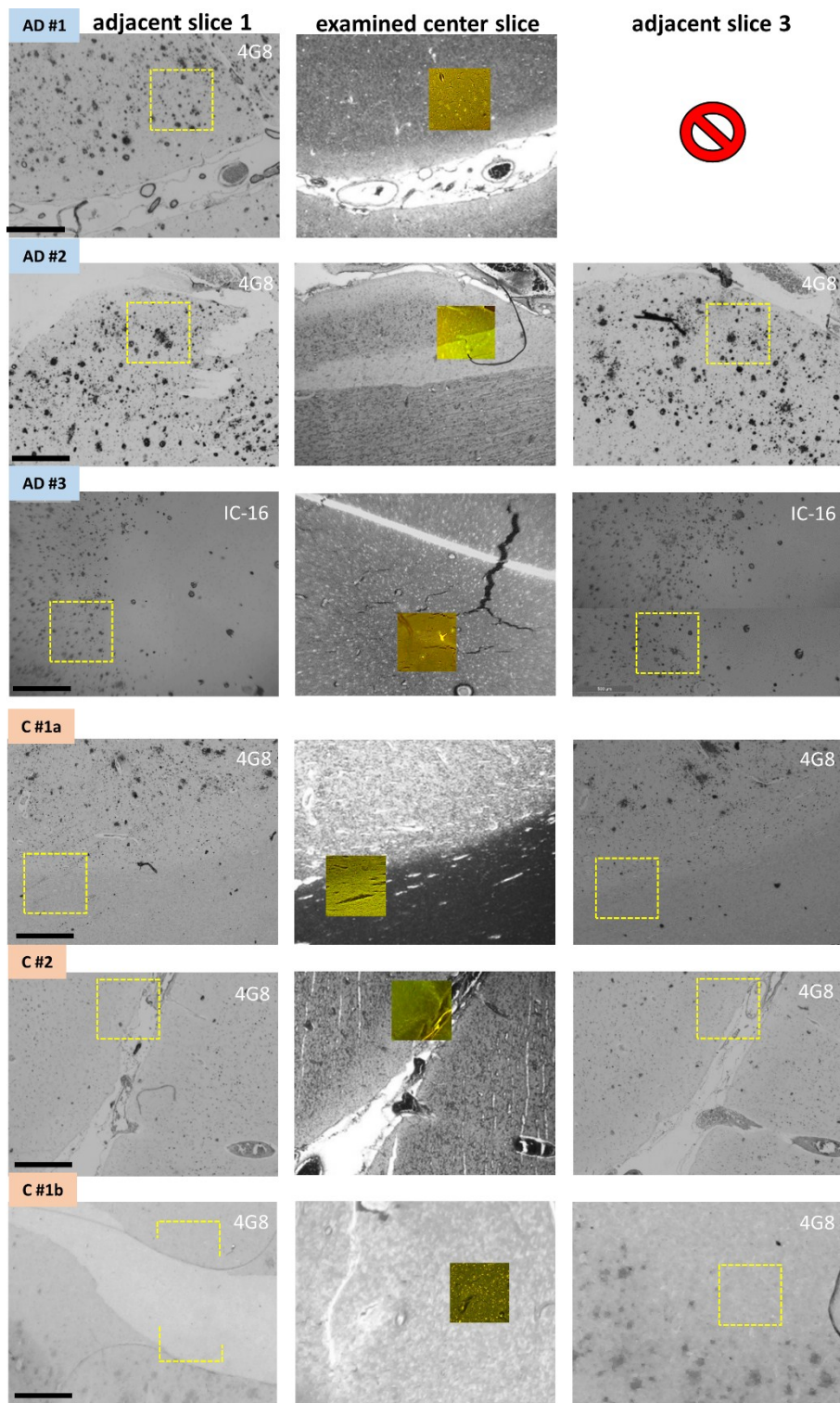


Figure S9: Overview of all sections measured in this study. Top three rows are the AD cases; the lower three cases the healthy control cases. The first and third column show the adjacent slices, stained either with 4G8 or with IC-16. Scale bars: 500 μm .

- 1 J. Jaumot, A. de Juan and R. Tauler, *Chemometrics and Intelligent Laboratory Systems*, 2015, **140**, 1–12.
- 2 MCR-ALS 2.0 toolbox, <https://mcrals.wordpress.com/download/mcr-als-2-0-toolbox/>.